**Application of Seasonal CRM Integrations to Develop Statistics and Improved GCM Parameterization of Subgrid Cloud-Radiation Interactions**
**Final Report**

**Principal Investigator:** Xiaoqing Wu, Department of Geological and Atmospheric Sciences, Iowa State University, 3010 Agronomy Hall, Ames, IA 50011, (515)294-9872 (phone), (515) 294-2619 (fax), wuxq@iastate.edu

**Co-Principal Investigator:** Xin-Zhong Liang, Illinois State Water Survey, Department of Natural Resources, University of Illinois at Urbana-Champaign, (217) 244-6864 (phone), (217) 244-0220 (Fax), xliang@uiuc.edu

## Abstract

The works supported by this ARM project lay the solid foundation for improving the parameterization of subgrid cloud-radiation interactions in the NCAR CCSM and the climate simulations. We have made a significant use of CRM simulations and concurrent ARM observations to produce long-term, consistent cloud and radiative property datasets at the cloud scale (Wu et al. 2006, 2007). With these datasets, we have investigated the mesoscale enhancement of cloud systems on surface heat fluxes (Wu and Guimond 2006), quantified the effects of cloud horizontal inhomogeneity and vertical overlap on the domain-averaged radiative fluxes (Wu and Liang 2005), and subsequently validated and improved the physically-based mosaic treatment of subgrid cloud-radiation interactions (Liang and Wu 2005). We have implemented the mosaic treatment into the CCM3. The 5-year (1979-1983) AMIP-type simulation showed significant impacts of subgrid cloud-radiation interaction on the climate simulations (Wu and Liang 2005). We have actively participated in CRM intercomparisons that foster the identification and physical understanding of common errors in cloud-scale modeling (Xie et al. 2005; Xu et al. 2005, Grabowski et al. 2005).

## 1. Background

The fundamental goal of the ARM program is ``to improve the treatment of radiation and clouds in the models used to predict future climate, particularly the general circulation models (GCMs)". In this project, we propose to apply seasonal integrations of NCAR cloud-resolving model (CRM) to develop cloud statistics and improved GCM parameterization of subgrid cloud-radiation interactions. Specifically, we propose to:

1) Conduct seasonal integrations using the NCAR CRM. We will focus on the Southern Great Plains (SGP) and the Tropical Western Pacific (TWP) sites, especially during multiple cloud regimes. The large-scale forcing data that drive the CRM include the ARM IOP measurements, the TOGA COARE (Tropical Ocean Global Atmosphere--Coupled Ocean Atmosphere Response Experiment) and GATE (Global atmospheric research program Atlantic Tropical Experiment) data, as well as NCEP/NCAR and ECMWF reanalysis. The CRM integrations will be evaluated against various observations, especially the ARM measurements of clouds and radiation budgets. This will establish the credibility of the CRM integrations to study subgrid cloud-radiation interactions.

2) Derive cloud statistics using the CRM integrations to characterize cloud geometric association (e.g., vertical overlapping and horizontal clustering) and optical property inhomogeneity (e.g., cloud liquid and ice distributions). These statistics will be in the form of probability distribution functions (PDFs) that are used by amosaic treatment to incorporate subgrid cloud-radiation interactions.

3) Implement the mosaic treatment with the CRM-based PDFs into the single-column model (SCM) of the NCAR Community Atmosphere Model (CAM). We will then conduct sensitivity experiments. These experiments will be used to fine-tune the mosaic treatment so that the results best match the ARM measurements and the CRM integrations. We will conduct the AMIP (Atmospheric Model Intercomparison Project) II integrations using the CAM with the improved scheme to quantify the climate impacts that result from subgrid cloud-radiation interactions.

## 2. Accomplishments from this ARM Project

The following is a list of the peer-reviewed journal articles that documented the outcomes of our previous project:


Wu, X., X.-Z. Liang, G.-J., Zhang 2003: Seasonal migration of ITCZ precipitation across the equator: Why can't GCMs simulate it? *Geophys. Res. Lett.*, **30**(15), 1824, doi:10.1029/2003GL017198.

Wu, X., and X.-Z. Liang, 2005: Radiative effects of cloud horizontal inhomogeneity and vertical overlap identified from a month-long cloud-resolving simulation. *J. Atmos. Sci.*, **62**, 4105-4112.

Xie, S., X. Wu, and Co-authors, 2005: Simulations of midlatitude frontal clouds by SCMs and CRMs during the ARM March 2000 cloud IOP. *J. Geophys. Res*., **110**, D15S03, doi:10.1029/2004JD005119.

Liang, X.-Z., and X. Wu, 2005: Evaluation of a GCM subgrid cloud-radiation interaction parameterization using cloud-resolving model simulations. *Geophys. Res. Lett.*, **32**, L06801, doi:10.1029/2004GL022301.

Wu, X., and X. Liang, 2005: Effect of subgrid cloud-radiation interaction on climate simulations, Geophys. Res. Lett., **32**, L24806, doi:10.1029/2005GL024432.

Xu, K.-M., X. Wu, and Co-authors, 2005: Modeling springtime shallow frontal clouds with cloud-resolving and single-column models. *J. Geophys. Res*., **110**, D15S03, doi:10.1029/2004JD005153.

Wu, X., and S. Guimond, 2006: Two- and three-dimensional cloud-resolving model simulations of the mesoscale enhancement of surface heat fluxes by precipitating deep convection. *J. Climate*, **19**, 139-149.

Grabowski, W.W., X. Wu, and Co-authors, 2006: Daytime convective development over land: A model intercomparison based on LBA observations. *Quart. J. Roy. Meteor. Soc*., **132**, 317-344.

Wu, X., and X.-Z. Liang, and S. Park, 2006: Cloud-resolving model simulations over the ARM SGP. *Mon. Wea. Rev., in press.*

Wu, X., S. Park, Q. Min, 2007: Seasonal variation of cloud systems over ARM SGP. Submitted to *J. Atmos. Sci*.

*2.1 CRM simulations of ARM cloud systems and quantification of radiative effects of cloud horizontal inhomogeneity and vertical overlap*

CRM simulations were performed over 26 days (June 22 – July 17) during the 1997 IOP at the SGP (Southern Great Plains) site, and validated against the concurrent ARM observations. CRM-simulated precipitation and cloud liquid water path are in general agreement with observations (Fig.1). Both longwave and shortwave radiative fluxes at TOA and surface are also consistent with the surface and satellite estimates. The differences between the CRM and observations are less than 5 $Wm^{-2}$ (Table 1).

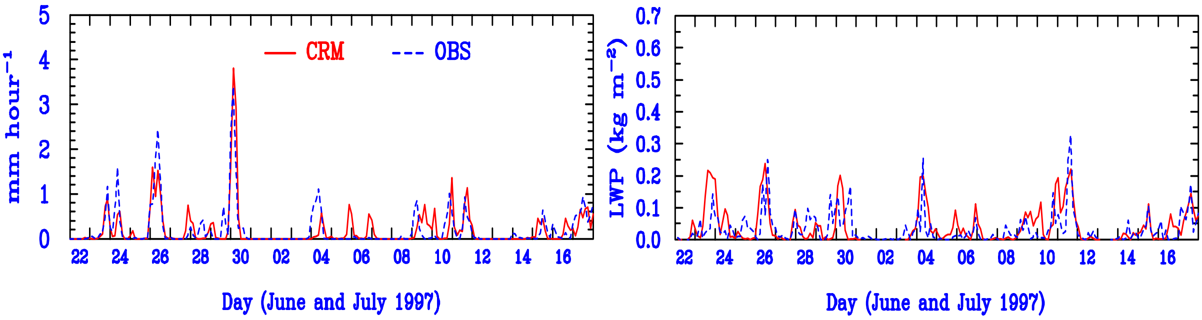


**Figure 1**. Left: Three-hourly domain-averaged surface rainfall rates (left) and cloudliquid water path (right) from the CRM (solid) and observations (OBS, dashed) over the SGP.

CRM-generated cloud distributions were then used in diagnostic calculations to quantify effects of horizontal condensate inhomogeneity and vertical cloud geometric overlap on the domain-averaged radiative fluxes and heating rates. These were accomplished by separating the condensate horizontal variability and cloud cover structure from the CRM output, which are either preserved or removed while conserving mass over the domain. Inadequate representation of these subgrid factors causes GCM underestimations of incoming shortwave (outgoing longwave) radiation by as much as 30 W $m^{-2}$ (Table 1); both condensate inhomogeneity and cloud geometric overlap effects are equally important, each accounting for approximately half of the GCM biases in TOA and surface radiative fluxes. This confirms the finding from the studies of TOGA COARE cloud systems (Wu and Moncrieff 2001).

**Table 1**. 26-day mean and standard deviation of longwave ($F_{LW}$) and shortwave ($F_{SW}$) radiative fluxes at the TOA and surface (SRF) from observations (OBS), CRM, GCM approach and diagnostic analysis (NCI). In GCM, the radiative transfer is calculated using in-cloud mean profiles of cloud liquid and ice water mixing ratio together with the mean temperature and moisture profiles, and the cloud vertical overlap is treated by the random overlap assumption because there is only one column for each time step. In NCI, the diagnostic analysis preserves the vertical structure of cloud cover geometry but has no condensate inhomogeneity.

| Radiative Fluxes ($Wm^{-2}$) | | Mean | | | | Deviation | | | |
|---|---|---|---|---|---|---|---|---|---|
| | | OBS | CRM | GCM | NCI | OBS | CRM | GCM | NCI |
| TOA | $F_{LW}$ | -259.5 | -261.8 | -233.9 | -249.5 | 26.6 | 26.2 | 45.7 | 34.9 |
| | $F_{SW}$ | 359.0 | 358.5 | 326.0 | 336.7 | 36.0 | 29.3 | 59.4 | 47.4 |
| SRF | $F_{LW}$ | -62.6 | -61.3 | -52.2 | -58.2 | 12.3 | 10.9 | 14.8 | 12.0 |
| | $F_{SW}$ | 253.8 | 258.6 | 223.9 | 234.6 | 42.1 | 31.9 | 64.8 | 52.0 |

*2.2 Evaluation of the mosaic representation of subgrid cloud-radiation interactions using CRM-derived cloud and radiation properties*

ARM-validated CRM simulations were used to evaluate the mosaic approach (Liang and Wang 1997) for the GCM parameterization of subgrid cloud-radiation interactions. CRM-generated cloud statistics determines the required characteristic structure differences between three primary cloud genera (convective, anvil and stratiform). These genera are evident in four major cloud clusters: deep clouds with the base below 5 km and the top reaching 10 km or higher; shallow clouds with the base below 5 km; middle-level clouds with the base between 5-10 km; and high-level clouds with the base above 10 km (Fig.2).

The mosaic approach with CRM cloud statistics faithfully simulates both the CRM domain-averaged radiative fluxes and the radiative heating rates. Both shortwave and longwave fluxes at the surface and TOA line closely with the CRM values (Fig.3). In contrast, the GCM approach substantially underestimates the incoming shortwave (outgoing longwave) radiations at the surface and TOA, accompanied with a great degree of scattering away from the CRM values. The mosaic approach reproduces the shortwave heating, longwave cooling, and total radiative rates below about 4 km and above 9 km (Fig. 4), while the GCM approach generates a systematic total heating (cooling) bias throughout the troposphere below (above) 9 km. The result indicates that the mosaic approach of the cloud overlap based on the cloud genera differing in formation mechanisms and of the optical inhomogeneity by cloud water path scaling can capture, respectively, the dominant effects of the cloud geometric association and optical property variability within a GCM grid.

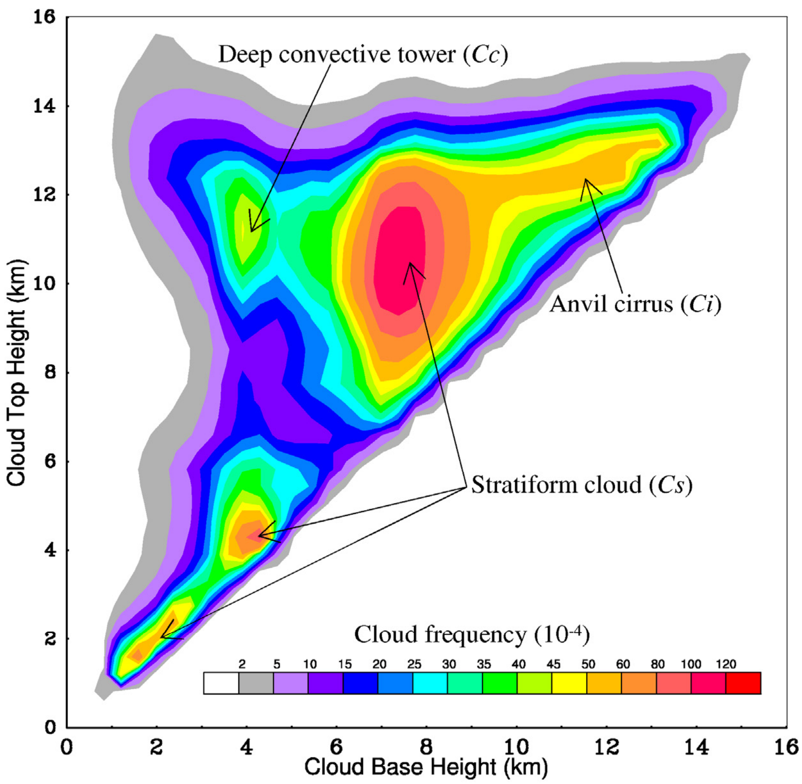


**Figure 2**. CRM simulated cloud frequency ($10^{-4}$) distribution as a function of the base and top heights. Three major cloud clusters are identified in the centers as *Cc*, *Ci*, and *Cs* that are distinguished by the mosaic approach.

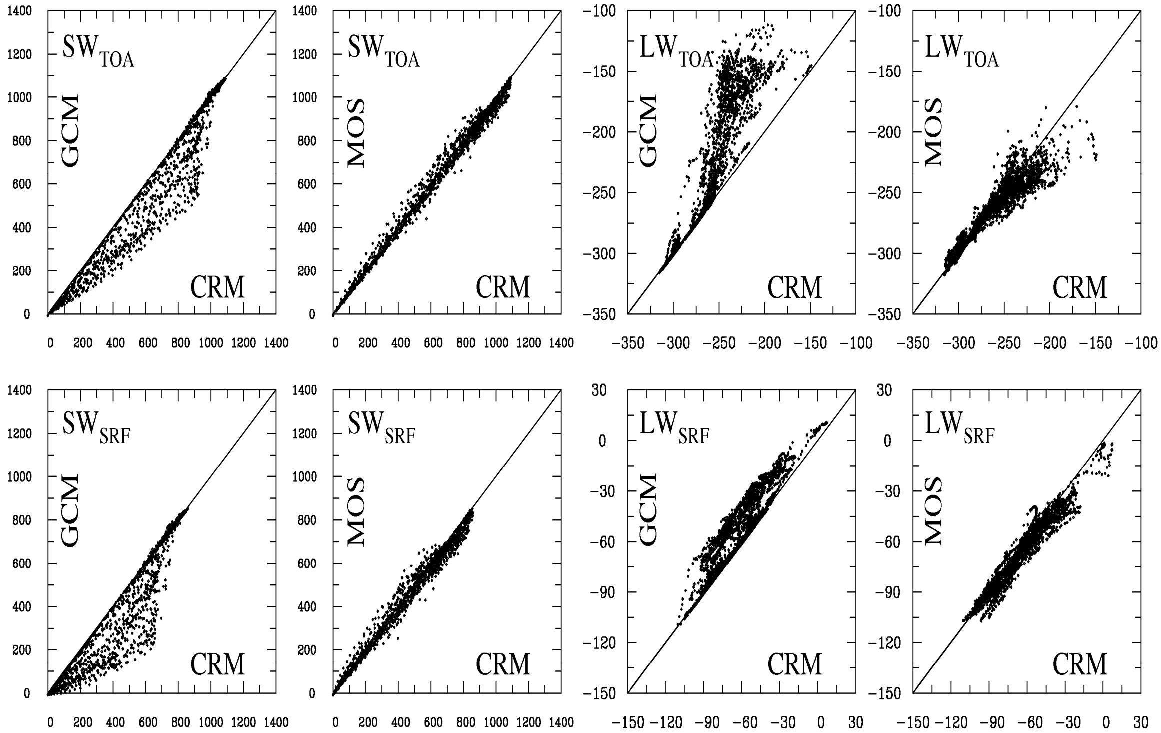


**Figure 3.** Scatter diagrams of the GCM and mosaic (MOS) approaches versus the CRM for longwave (LW) and shortwave (SW) net fluxes (W $m^{-2}$) at the surface (SRF) and TOA. Downward fluxes are positive and each point denotes a 15-minute sample.

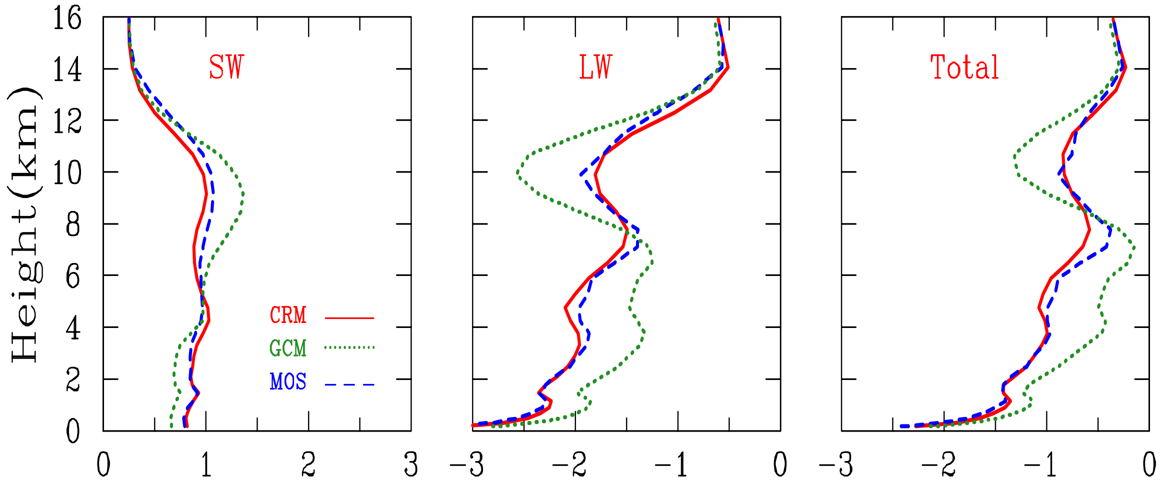


**Figure 4**. Domain average longwave (LW), shortwave (SW) and total heating rate (Kday$^{-1}$) profiles as calculated by the CRM, GCM and mosaic (MOS) approaches.

*2.3 Impacts of subgrid cloud-radiation interaction on CCM3 AMIP simulations*

Improved mosaic treatment of subgrid cloud-radiation interactions was implemented into the CCM3. The initial 5-year (1979-1983) AMIP simulations prescribed with the observed SST showed encouraging results. In particular, the mosaic treatment produces smaller radiation-effective clouds than the random overlap assumption. This facilitates removal of the necessity to use unrealistic cloud amount and cloud water contents in order to maintain the global radiation budget closer to satellite observations in the standard CCM3 simulation. Sensitivity experiments with modified cloud parameterizations showed that the mosaic approach enables the use of more realistic cloud amounts *as well as* cloud water contents (Fig.5) in producing net radiative fluxes closer to observations (Fig.6). This leads to a significantly different radiative heating rate; consequently, not only the representation of cloud-radiation interaction is more physically consistent and accurate, but also mean climate variables, such as the temperature field, are better simulated over the tropical upper troposphere and overall are closer to reanalysis and observational data (Fig.7). The global annual mean precipitation rates from the mosaic and the standard CCM3 simulations are 2.97 and 3.10 mm day$^{-1}$, as compared to 2.69 mm day$^{-1}$ in observations.

The CCM3 study was our first attempt to explore the impact of subgrid cloud-radiation interactions on climate simulations. We made adjustments to the diagnostic scheme of cloud cover and the prescribed scale factor of cloud water content to obtain global mean values close to the observed ISCCP (International Satellite Cloud Climatology Project) cloud amounts and SSM/I (Special Sensor Microwave/Imager) liquid water paths. The main purpose of this experiment was to demonstrate that the mosaic treatment enables the incorporation of cloud amounts and water paths that are consistent with observations while maintaining the global radiation budget close to observations. As such, questions were raised regarding the feedback processes that may explain the resulting large climate responses when the mosaic approach is compared with the standard CCM3. Further analysis and sensitivity experiments are required to understand the physical processes involved in the climate responses to the improved radiation scheme.

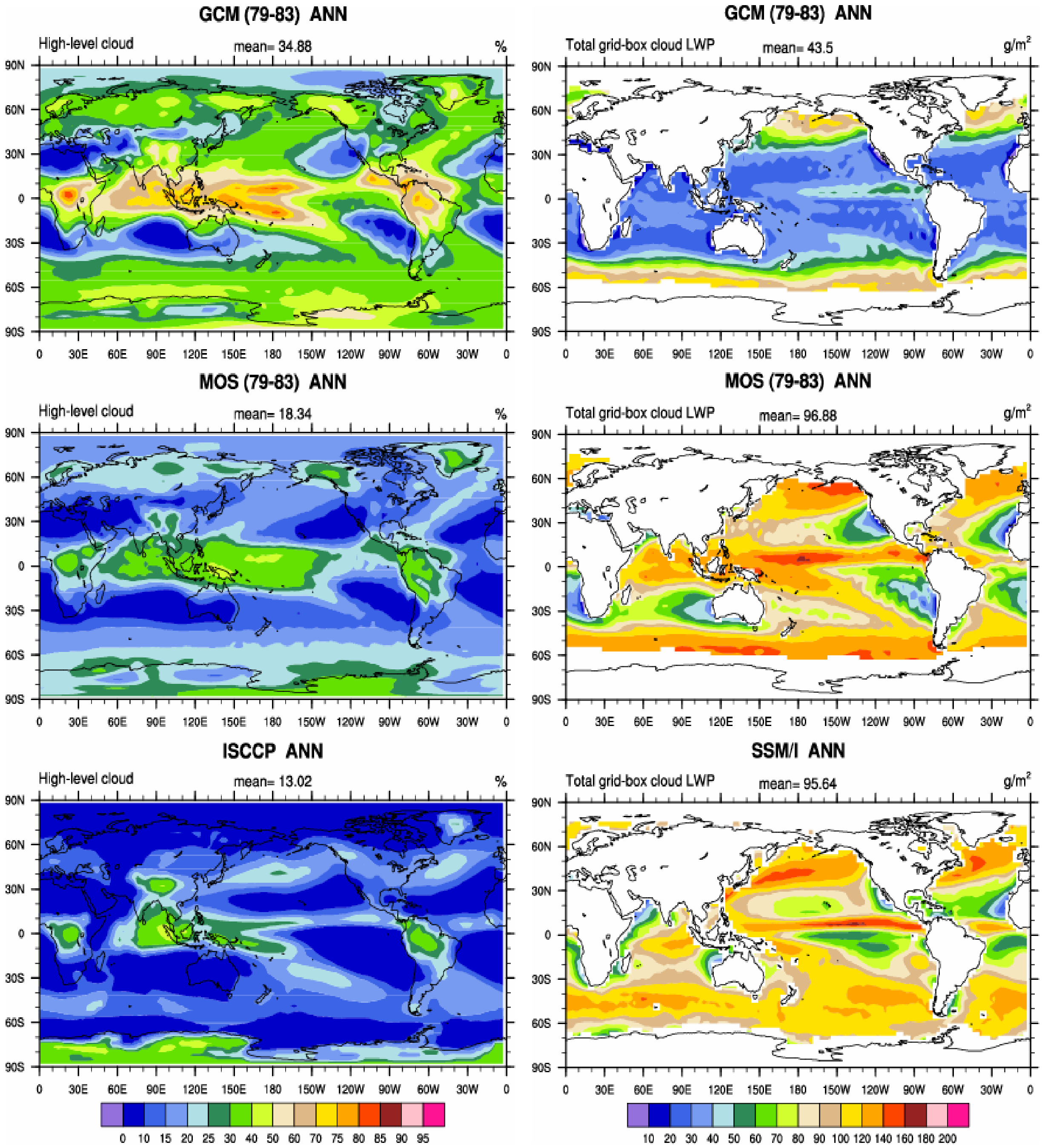


**Figure 5**. Left: 5-year (79-83) averages of high-level cloud fraction (percent) from CCM3 (GCM, top), mosaic run (MOS, middle), and ISCCP (bottom). Right: 5-year averages of total cloud liquid water path ($gm^{-2}$) from CCM3 (GCM, top), mosaic run (MOS, middle), and SSM/I (bottom).

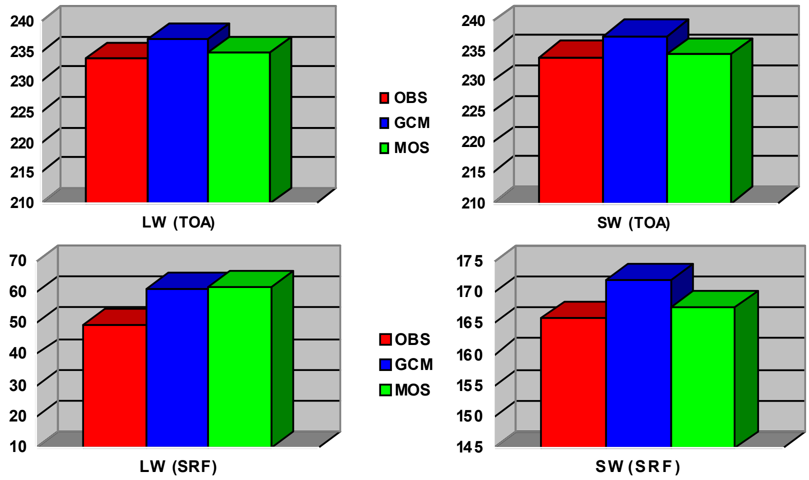


**Figure 6**. 5-year global averages of radiative fluxes ($Wm^{-2}$) from observations (OBS), CCM3 (GCM) and mosaic run (MOS).

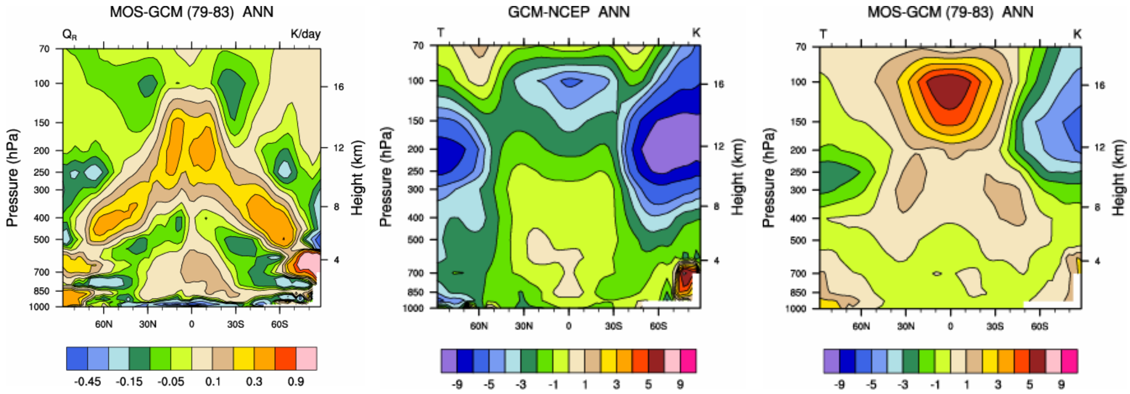


**Figure 7**. 5-year zonal average of the difference of radiative heating rate ($Kday^{-1}$) between mosaic run (MOS) and GCM (left), the differences of temperature (K) between GCM and NCEP (middle) and between MOS and GCM (right).